MOLECULAR AND CELLULAR BIOLOGY, Oct. 1997, p. 6139–6146 Vol. 17, No. 10
0270-7306/97/$04.00+0

VP16 Targets an Amino-Terminal Domain of HCF Involved in Cell Cycle Progression

ANGUS C. WILSON,[1]† RICHARD N. FREIMAN,[1,2] HIROSHIGE GOTO,[3] TAKEHARU NISHIMOTO,[3] AND WINSHIP HERR[1]*

Cold Spring Harbor Laboratory, Cold Spring Harbor, New York 11724[1]; Genetics Program, State University of New York, Stony Brook, New York 11794[2]; and Department of Molecular Biology, Medical Institute of Bioregulation, Graduate School of Medical Science, Kyushu University, 3-1-1 Maidashi, Higashi-ku, Fukuoka 812, Japan[3]

Received 15 May 1997/Returned for modification 19 June 1997/Accepted 30 June 1997

The herpes simplex virus (HSV) regulatory protein VP16 activates HSV immediate-early gene transcription through formation of a multiprotein-DNA complex on viral promoters that includes the preexisting nuclear proteins HCF and Oct-1. The HCF protein is a complex of amino- and carboxy-terminal polypeptides derived from a large (~2,000-amino-acid) precursor by proteolytic processing. Here we show that a 361-residue amino-terminal region of HCF is sufficient to bind VP16, stabilize VP16-induced complex assembly with Oct-1 and DNA, and activate transcription in vivo. This VP16 interaction region contains six kelch-like repeats, a degenerate repeat motif that is likely to fold as a distinctive β-propeller structure. The third HCF kelch repeat includes a proline residue (P134) that is mutated to serine in hamster tsBN67 cells, resulting in a temperature-sensitive defect in cell proliferation. This missense mutation also prevents direct association between HCF and VP16, suggesting that VP16 mimics a cellular factor required for cell proliferation. Rescue of the tsBN67 cell proliferation defect by HCF, however, requires both the VP16 interaction domain and an adjacent basic region, indicating that HCF utilizes multiple regions to promote cell cycle progression.

Lytic infection by herpes simplex virus (HSV) is characterized by a cascade of sequential gene expression initiated by the virion protein VP16. Upon infection, VP16 (also known as Vmw65 or αTIF) is released into the cell, whereupon it promotes the formation of a multiprotein-DNA complex with two cellular factors, HCF (also known as C1, VCAF, or CFF) and Oct-1. VP16 associates with HCF independently of DNA (14, 17, 44), which stabilizes the association of VP16 with Oct-1 on VP16-responsive *cis*-regulatory sites — the TAATGARAT element — within the HSV immediate-early promoters (11, 15). The formation of this VP16-induced complex initiates the cascade of HSV gene expression (reviewed in references 25 and 33).

In human cells, HCF comprises a family of 110- to 150-kDa polypeptides (18, 39) derived from a 2,035-amino-acid precursor protein (HCF_{300}) through proteolytic processing: cleavage at any one of a series of six centrally located 26-amino-acid repeats, called the HCF repeats, results in amino- and carboxy-terminal HCF fragments which remain associated after cleavage (16, 39, 41).

Although the precise cellular function of HCF has not been established, analysis of a temperature-sensitive hamster cell line, called tsBN67 (24), has revealed that HCF is required for cell proliferation (12). At the nonpermissive temperature, tsBN67 cells undergo a G_0/G_1 cell cycle arrest, which is due to a proline-to-serine substitution at position 134 (P134S) in the amino-terminal region of HCF (12). HCF stability and processing are not affected by the tsBN67 mutation, but VP16-induced complex formation and VP16 activation of transcription are both disrupted at the nonpermissive temperature (12). Whether the defect in VP16 activity is due to a direct effect on the VP16-HCF interaction or an indirect effect due to the cell cycle arrest of the tsBN67 cells at the nonpermissive temperature is not known.

Here, we show that VP16 interacts with a discrete amino-terminal 361-amino-acid region of HCF that is likely to form a β-propeller structure. This region, called the HCF_{VIC} domain, is sufficient to promote VP16-induced complex formation in vitro and transcriptional activation by VP16 in vivo. The tsBN67 point mutation lies within the HCF_{VIC} domain and prevents interaction with VP16. Thus, the same point mutation in HCF disrupts both cell cycle and VP16 function, suggesting that VP16 interacts with the cell cycle machinery to regulate HSV gene expression.

MATERIALS AND METHODS

Mammalian expression plasmids. T7-epitope-tagged VP16 (residues 5 to 412) lacking the carboxy-terminal activation domain was expressed from pCGTVP16ΔC. This construct is equivalent to pCGNVP16ΔC (39), except that the amino-terminal HA epitope tag was replaced by the sequence MASMTG GQQMG, which corresponds to the first 11 residues of the bacteriophage T7 gene 10 capsid protein and is recognized by the anti-T7 (αT7) tag monoclonal antibody (Novagen).

The epitope-tagged full-length HCF expression construct $pCGNHCF_{FL}$ has been described previously (39). $pCGNHCF_{N1011}$ encodes the first 1,011 residues of HCF with an additional *Bgl*II linker sequence, encoding residues Arg-Ser, before the stop codon. $pCGNHCF_C$ encodes residues 1436 to 2035 and contains the *Bgl*II site. The coding sequences of $pCGNHCF_{N1011}$ and $pCGNHCF_C$ were fused at the engineered *Bgl*II site to give $pCGNHCF_{\Delta rep}$, encoding a product in which residues 1012 to 1435 are replaced by residues Arg-Ser. Additional truncations were generated by using appropriate restriction sites or oligonucleotide-mediated mutagenesis. The sequences of PCR-generated fragments were verified by DNA sequence analysis.

Transfections, immunoprecipitations, and immunoblotting. Human 293 cells were transfected by electroporation with a Bio-Rad Genepulser with Extendor, set at 200 mV and 960 μF. Whole-cell nuclear extracts were prepared after 40 h by lysing cells in medium-salt lysis buffer (250 mM KCl, 10 mM HEPES-KOH [pH 7.9], 5% glycerol, 0.25% Nonidet P-40, 0.2 mM EDTA, 0.5 mM phenylmethylsulfonyl fluoride, 0.2 mM sodium vanadate, 50 μM sodium fluoride, 1 mM dithiothreitol, 1 mM benzamidine, 10 mg of leupeptin per ml, 10 mg of aprotinin per ml). Nuclei were extracted at 4°C for 30 min and removed by centrifugation. For immunoprecipitations, 300 μl of extract was incubated with 5 μl of anti-

* Corresponding author. Mailing address: Cold Spring Harbor Laboratory, P.O. Box 100, Cold Spring Harbor, NY 11724. Phone: (516) 367-8401. Fax: (516) 367-8454. E-mail: herr@cshl.org.

† Present address: Department of Microbiology and Kaplan Cancer Center, New York University School of Medicine, New York, NY 10016.

hemagglutinin (αHA) antibody (12CA5)-coupled protein G-agarose beads at 4°C for 1 h. The beads were washed four times with 1 ml of lysis buffer before separation by sodium dodecyl sulfate (SDS)-polyacrylamide gel electrophoresis. Immunoblotting was performed as described in reference 39 and detected by enhanced chemiluminescence (Amersham). The αT7 tag monoclonal antibody (Novagen) was diluted 1:10,000.

In vitro transcription and translation, electrophoretic mobility retardation, and coimmunoprecipitation assays. Template fragments for cell-free expression of non-epitope-tagged amino-terminal HCF polypeptides were generated by PCR with an upstream primer that included a T7 RNA polymerase promoter and rabbit β-globin translation initiation sequence (5′ATTAATACGACTCAC TATAGGAAACAGACACCA**ATG**. . . . .3′ [the translation initiation codon is boldfaced]). Sequences encoding the carboxy terminus of HCF were subcloned into the in vitro transcription and translation expression plasmid pCITE2a+ (Novagen) to give pCITEHCF$_C$. For in vitro translation of HA-tagged VP16ΔC and VP16ΔC-E361A/385Ala3 (21), VP16 sequences (encoding residues 5 to 412) were subcloned into pNCITE (a gift of W. Tansey), a derivative of pCITE that includes the HA epitope at the amino terminus of the expressed protein. The P134S mutation was engineered in human HCF by site-directed mutagenesis.

In vitro transcription and translation reactions were performed in the presence of [^{35}S]methionine by using the TNT system and protocol (Promega, Inc.). HA-epitope-tagged polypeptides were labeled to a lower specific activity by including 1/20 of the standard amount of [^{35}S]methionine. The amount of full-length translation product was determined with a Fuji BAS1000 phosphorimager after SDS-polyacrylamide gel electrophoresis, and, where necessary, normalized by addition of unprogrammed lysate.

Electrophoretic mobility retardation assays were performed as described previously (39); complex formation was performed at 30°C, and electrophoresis was performed at room temperature. Coimmunoprecipitation assays of in vitro-translated proteins were performed as follows. Prior to immunoprecipitation, the HA-tagged (5 μl) and untagged (10 μl) polypeptides were mixed and incubated at room temperature for 15 min. Then 5 μl of precoupled αHA (12CA5)-protein G-agarose beads was added in 35 μl of buffer D/0.2 (10 mM Tris-HCl [pH 7.9], 200 mM KCl, 0.1% Nonidet P-40, 5% glycerol, 1 mM EDTA, 0.5 mM phenylmethylsulfonyl fluoride, 50 μM sodium fluoride, 0.5 mM sodium vanadate, 10 mg of leupeptin per ml, 10 mg of aprotinin per ml) and mixed, and the mixture was incubated for a further 1 h at room temperature with occasional stirring. After incubation, the beads were washed four times with 1 ml of buffer D/0.2. Immune complexes were resolved by SDS-polyacrylamide gel electrophoresis (12% polyacrylamide), treated with the enhancing agent Amplify (Amersham), and visualized by fluorography.

Yeast reporter strains and expression constructs. *Saccharomyces cerevisiae* W3031a (32) was used to engineer two HIS3 reporter strains. Briefly, six copies of an ICP0 (OCTA$^+$)TAATGARAT element (CATGCTAATGATATTCTT), spaced by *Xho*I recognition sites, was ligated into the *Eco*RI site of plasmid pTH1 (5) (a gift of G. Mandel) upstream of the GAL1 promoter. This plasmid and unmodified pTH1 were linearized with *Pvu*II, transformed into W3031a, and grown on plates lacking uracil. Ura$^+$ colonies were selected and then restreaked in the presence of 5-fluoroorotic acid (2), and eight 5-fluoroorotic acid-resistant colonies were screened by Southern hybridization with a HIS3-specific probe to recover strains that had lost the URA3 marker but retained the HIS3 reporter. These reporter strains were then transformed with low-copy-number CEN vectors (1) expressing HA epitope-tagged Oct-1 POU domain (residues 280 to 439), full-length VP16 (residues 5 to 490), and HCF$_{N380}$ containing TRP1, LEU2, and URA3 selectable markers, respectively. Transformants were selected at 30°C on plates lacking tryptophan, leucine, and uracil, and activation of the HIS3 reporter was assayed on similar plates lacking histidine as well.

Rescue of the tsBN67 temperature-sensitive defect. tsBN67 cells (2×10^5/dish) were incubated at 33.5°C for 20 h and transfected with 2 μg of each HCF expression plasmid and 2 μg of pSV2neo by the Chen and Okayama method as described previously (37). At 20 h after transfection, the cells were washed in TD buffer and incubated at 33.5°C for an additional 48 h, and transformants were selected over 2 weeks at either 33.5 or 39.5°C (two plates of each) in the presence of G418 (0.8 mg/ml).

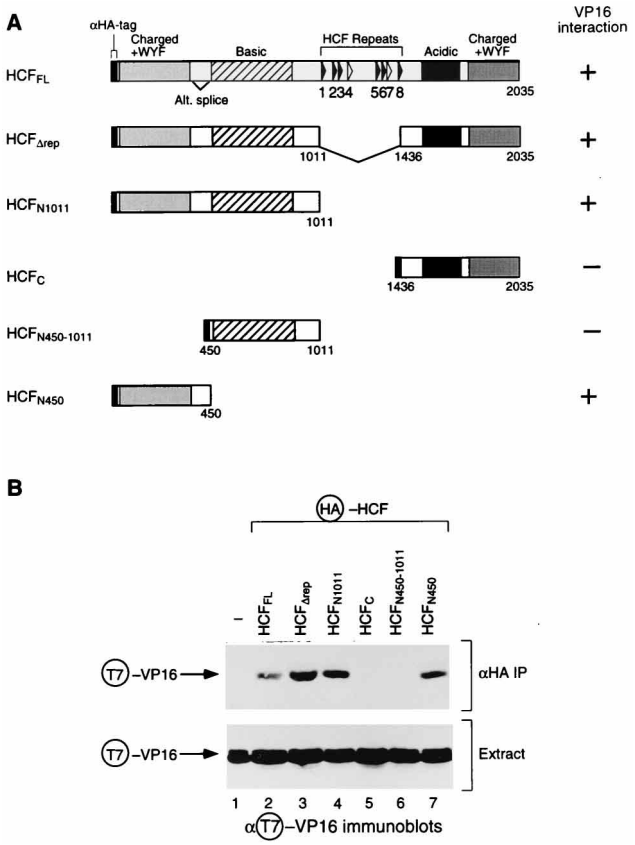

FIG. 1. VP16 associates with the first 450 residues of HCF. (A) The structures of recombinant HCF and its derivatives are shown schematically. The six near-perfect HCF repeats (solid arrowheads) and two degenerate repeats (open arrowheads) are indicated. Regions generally enriched in particular types of amino acids are represented by boxes. WYF signifies tryptophan, tyrosine, and phenylalanine. The position of the alternative splice (Alt. splice) that removes residues 382 to 450 is shown. In HCF$_{\Delta rep}$, residues 1012 to 1435 are deleted, removing the HCF repeats. The polypeptide HCF$_{N1011}$ includes all residues amino-terminal to HCF repeat 1 (residues 1 to 1011), whereas HCF$_C$ includes all residues carboxy-terminal to HCF repeat 8 (residues 1436 to 2035). Each polypeptide includes an amino-terminal αHA epitope tag. The ability or inability of each HCF polypeptide to coimmunoprecipitate VP16 is indicated by (+) and (−), respectively. (B) HCF-VP16 coimmunoprecipitation. Extracts were prepared from 293 cells transfected with 5 μg of T7-epitope tagged VP16ΔC expression plasmid alone (lane 1) or cotransfected with 5 μg of expression plasmids encoding HA epitope-tagged HCF$_{FL}$, HCF$_{\Delta rep}$, HCF$_{N1011}$, HCF$_C$, HCF$_{N450–1011}$, and HCF$_{N450}$ (lanes 2 to 7). In the top panel, tagged HCF proteins were recovered by immunoprecipitation with the αHA monoclonal antibody, resolved on an SDS-8% polyacrylamide gel and immunoblotted with the αT7 tag antibody to detect coimmunoprecipitated VP16. In the lower panel, 1/10 of the starting extract was probed directly.

RESULTS

VP16 associates with a discrete region at the amino terminus of HCF. Figure 1A (top) shows a schematic of the structure of epitope-tagged HCF. In our initial characterization of HCF (39), we noted a series of 26-amino-acid sequence repeats (the HCF repeats), which have since been shown to be responsible for directing processing of HCF (41). We also noted four regions of HCF that displayed significant enrichment for particular amino acids, i.e., (i) amino- and carboxy-terminal regions enriched for charged residues and large hydrophobic residues (phenylalanine, tyrosine, and tryptophan), and (ii) central regions enriched in basic or acidic residues (Fig. 1A).

HCF binds to VP16 and stabilizes the VP16-induced complex. We mapped the region of HCF responsible for binding to VP16 by coimmunoprecipitation of HCF and VP16 polypeptides after transient expression in human 293 cells. Figure 1A shows the HCF truncations used in this experiment. The HCF polypeptides were tagged with an HA epitope (HA-HCF), and VP16 was tagged with a bacteriophage T7 gene 10 epitope (T7-VP16). HA-tagged HCF polypeptides were recovered by immunoprecipitation with an αHA monoclonal antibody, and the resulting immune complexes were resolved by SDS-polyacrylamide gel electrophoresis. Coimmunoprecipitated VP16 was then detected by immunoblotting with an αT7 antibody.

Figure 1B shows the results of such an experiment. Prior to HA-HCF immunoprecipitation, each extract contained similar

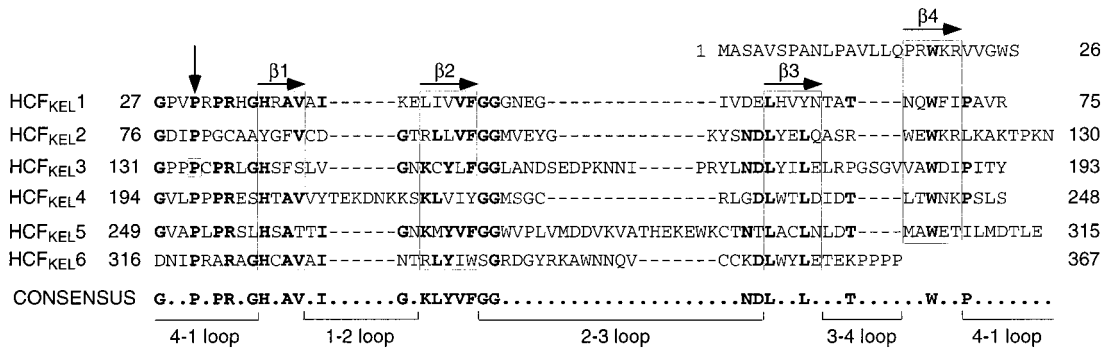

FIG. 2. The HCF$_{VIC}$ domain is composed of six kelch-like repeats. The alignment of the six kelch-like repeats found at the amino terminus of HCF is shown. Following the structure of galactose oxidase (3, 13), each kelch-like repeat is made up of four β-strands (β1 to β4 [boxed]) that form a β-sheet or blade. The β-strands are connected by loops of variable length (1-2, 2-3, 3-4, and 4-1), with the 4-1 loop connecting the individual blades. In all known β-propeller structures, the last blade is composed of three β-strands derived from the last repeat unit and one β-strand that lies amino-terminal to the first repeat unit. Residues conserved in three or more repeats are shown in boldface type. The proline residue (P134) that is mutated to serine in hamster tsBN67 HCF is boxed and corresponds to an otherwise invariant position indicated by a vertical arrow. The wild-type hamster HCF sequence in this region is identical to human HCF except for a single conservative aspartic-acid-to-glutamic-acid substitution at position 238.

levels of T7-VP16 (Fig. 1B, lower panel). After immunoprecipitation, however, the levels of T7-VP16 differed (upper panel). VP16 was not recovered in the absence of HA-HCF expression but was recovered in the presence of full-length HA-HCF (compare lanes 1 and 2), indicating that recovery of VP16 was dependent on HA-HCF expression. Association of HCF and VP16 in this assay is resistant to high concentrations (400 μg/ml) of the DNA-binding inhibitor ethidium bromide (20, 42), consistent with DNA-independent HCF association with VP16.

Deletion of the HCF repeats did not disrupt association with T7-VP16 (compare lanes 2 and 3), indicating that HCF processing is not required for its association with VP16. Of the remaining four HA-HCF truncations analyzed, those carrying the amino-terminal 450 residues of HCF associated with T7-VP16 (lanes 4 and 7), whereas those lacking the amino-terminal 450 residues failed to associate with T7-VP16 (lanes 5 and 6). These results indicate that the amino-terminal 450 residues of HCF are sufficient to bind VP16.

The amino-terminal region of HCF contains six kelch-like sequence repeats. The amino-terminal 450 amino acids of HCF encompass the amino-terminal region enriched in charged and large hydrophobic residues (Fig. 1A). Closer examination of this sequence revealed within the first 380 residues six copies of a sequence motif similar to a degenerate 50- to 65-residue repeat motif found in a diverse array of proteins including the *Drosophila* egg chamber protein kelch (45), the *Limulus* actin-binding protein scruin (38), the *Caenorhabditis* spermatid formation protein SPE-26 (35), and an actin kinase (8). This repeat motif has been variously termed the kelch or GG repeat; we refer to the six repeats in HCF as kelch repeats HCF$_{KEL}$1 to HCF$_{KEL}$6. Figure 2 shows an alignment of the six HCF$_{KEL}$ repeats.

Comparison of kelch repeat-containing proteins (3) indicates that each repeat, except for the last one, forms a four-stranded (β1 to β4) β-sheet that comes together to form a highly distinctive barrel-like structure resembling a propeller. This structure is variously referred to as a β-propeller (34) or superbarrel (4). The last repeat in known β-propellers contains only three β strands (β1 to β3) (Fig. 2) and associates with a fourth β strand provided by the amino terminus of the circular β-propeller structure, thus stabilizing the structure (reviewed in reference 29). The sequence similarity to other kelch repeat-containing proteins suggests that the six HCF$_{KEL}$ repeats within the first 380 residues of HCF form a six-bladed β-propeller structure.

The putative amino-terminal β-propeller domain of HCF is sufficient to bind VP16. To determine how the six HCF$_{KEL}$ repeats relate to the ability of HCF to bind VP16, we assayed HCF association with VP16 by using a more extensive set of truncations within this region of HCF, as shown in Fig. 3. As in Figure 1, we assayed HCF binding to VP16 in a coimmunoprecipitation assay, but in this case we assayed the recovery of untagged HCF with immunoprecipitated HA-tagged VP16 (HA-VP16). Some of the HCF truncations were predicted to disrupt the putative β-propeller structure and thus perhaps affect the stability of the proteins. Therefore, here, both the HCF and HA-VP16 proteins were expressed by translation in vitro, such that protein synthesis could be controlled and monitored more easily. To avoid obscuring the coimmunoprecipitated HCF proteins, the VP16 was labelled at 1/20 the specific activity of HCF (see Materials and Methods). To monitor the selectivity of HCF association with VP16, we compared recovery of HCF with VP16 and a matched VP16 mutant carrying four point mutations that selectively disrupt the association of HCF with VP16 (E361A/385A1a3) (21). Using this assay, we measured the binding of four further truncations of HCF.

Some forms of natural HCF lack residues 382 to 450 owing to an alternatively spliced mRNA (39); this natural HCF deletion disrupts the association between amino-terminal and carboxy-terminal HCF fragments following HCF processing (41). We therefore asked whether HCF residues 1 to 380 (HCF$_{N380}$), which span the six HCF$_{KEL}$ repeats as shown in Fig. 3A and thus contain the putative β-propeller structure but lack sequences important for HCF fragment coassociation, can bind VP16. The results of this experiment are shown in Fig. 3B (lanes 1 to 3). HCF$_{N380}$ was recovered by coimmunoprecipitation with wild-type HA-VP16 (lane 2) but was not recovered if either HA-VP16 was absent in the reaction (lane 1) or the HA-VP16 mutant was used in the coimmunoprecipitation (lane 3). Thus, HCF$_{N380}$ can bind VP16 and amino- and carboxy-terminal HCF fragment coassociation is apparently not required for HCF binding to VP16.

To determine the requirement for the HCF$_{KEL}$ repeat region for HCF binding to VP16, we assayed the three other truncations of HCF: HCF$_{N345}$ removes the last predicted β strand of HCF$_{KEL}$6; and HCF$_{N20–450}$ and HCF$_{N51–450}$ truncate the amino terminus of HCF without or with the loss of a

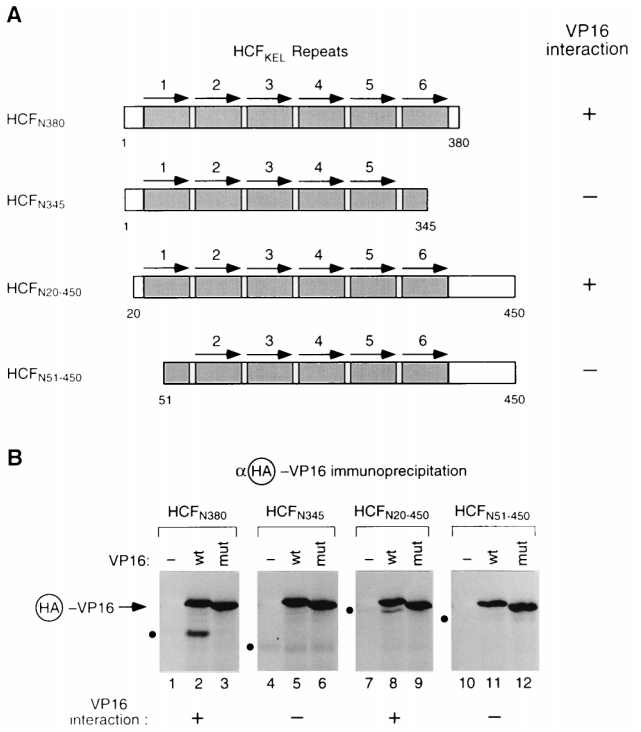

FIG. 3. The HCF$_{KEL}$ repeats are sufficient and required for the association of HCF with VP16. (A) Structure of amino-terminal HCF polypeptides used for coimmunoprecipitation. Shaded boxes denote the HCF$_{KEL}$ repeats. + and − denote the ability or inability to associate with VP16 in the coimmunoprecipitation assay, respectively. (B) Coimmunoprecipitation of HCF polypeptides with αHA epitope-tagged VP16. The proteins were translated in vitro with [^{35}S]methionine, allowed to associate, and then recovered by immunoprecipitation with αHA monoclonal antibody beads. To compensate for the relative inefficiency of recovery of untagged protein (approximately 10%), the epitope-tagged VP16 polypeptides were labeled to 1/20 of the specific activity of the untagged polypeptides. Each HCF polypeptide was mixed with a mock lysate (lanes 1, 4, 7, and 10), with HA-tagged wild-type VP16 (lanes 2, 5, 8, and 11), or with HA-tagged mutant VP16-E361A/385Ala3 (lanes 3, 6, 9, and 12). The HCF polypeptides were as follows: HCF$_{N380}$ (lanes 1 to 3), HCF$_{N345}$ (lanes 4 to 6), HCF$_{N20–450}$ (lanes 7 to 9), HCF$_{N51–450}$ (lanes 10 to 12). Immune complexes were resolved on an SDS-12% polyacrylamide gel and detected by fluorography. The mobility of each HCF polypeptide is denoted by a dot; successful (+) or unsuccessful (−) recovery of the HCF polypeptide by wild-type VP16 is indicated at the bottom of the figure.

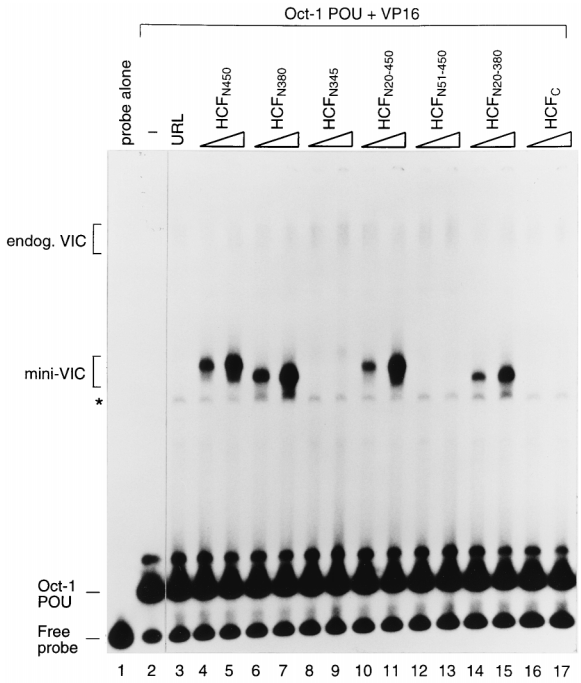

FIG. 4. The HCF$_{KEL}$ repeats are sufficient and required for HCF stabilization of the VP16-induced complex. Polypeptides derived from the amino- and carboxy-terminal regions of HCF were synthesized in vitro and assayed for HCF activity in an electrophoretic mobility retardation assay, with a labeled (OCTA^{+})TAATGARAT probe. Unbound probe (lane 1), probe mixed with Oct-1 POU domain and GST-VP16 (lane 2), and Oct-1 POU domain and GST-VP16 with 3 μl of unprogrammed reticulocyte lysate (lane 3) are shown. The remaining lanes show assays with either 1 μl (lanes 4, 6, 8, 10, 12, 14, and 16) or 3 μl (lanes 5, 7, 9, 11, 13, 15, and 17) of lysates programmed with templates for expression of the HCF molecules indicated above the lanes. The positions of the free probe, Oct-1 POU-domain complex, and the VP16-induced complex containing rabbit HCF from the lysates (endog. VIC) or truncated HCF fragments (mini-VIC) are indicated. The asterisk indicates a weak HCF-independent VP16-Oct-1 POU domain complex (see lane 2).

portion of HCF$_{KEL}$1, respectively. Consistent with the HCF$_{KEL}$ repeats being important for VP16 binding, both HCF$_{N345}$ and HCF$_{N51–450}$ failed to associate effectively with VP16 (Fig. 3B, lanes 5 and 11). In contrast, the small amino-terminal truncation HCF$_{N20–450}$ could still associate with VP16, although somewhat less effectively (lane 8). The reduced but still significant recovery of HCF$_{N20–450}$ may result from partial disruption of the very amino terminus of the first predicted β strand in the putative β-propeller structure. These results indicate that the entire HCF$_{KEL}$-repeat region is both sufficient and required for effective HCF binding to VP16.

The putative amino-terminal β-propeller region of HCF is sufficient to stabilize VP16-induced complex formation. In addition to binding to VP16, HCF stabilizes the VP16-induced complex. To determine whether the sequences required for HCF stabilization of the VP16-induced complex colocalize with those required for VP16 binding, we assayed the various HCF truncations in a VP16-induced complex assay. Figure 4 shows the results of this analysis. VP16-induced complex formation was assayed by electrophoretic mobility retardation on a VP16-responsive TAATGARAT element, with *Escherichia coli*-expressed Oct-1 POU domain and VP16 and in vitro-translated HCF proteins. Consistent with the VP16-binding results, the amino-terminal HCF$_{N450}$ fragment, but not the carboxy-terminal HCF$_{C}$ fragment, promoted VP16-induced complex formation (Fig. 4, compare lanes 4 and 5 and lanes 16 and 17 with lane 3). Thus, the amino-terminal region of HCF is sufficient to stabilize the VP16-induced complex.

Analysis of the remaining truncations of the amino-terminal region of HCF exhibited a complete correspondence between the ability to bind VP16 (Fig. 3) and stabilize the VP16-induced complex. Thus, HCF$_{N380}$ and HCF$_{N20–450}$, but not HCF$_{N345}$ and HCF$_{N51–450}$, were active in the VP16-induced complex formation assay (Fig. 4, compare lanes 6 to 13). Furthermore, assay of the combined truncation HCF$_{N20–380}$ (lanes 14 and 15) shows that this minimal 361-amino-acid HCF$_{KEL}$ repeat region of HCF is sufficient to stabilize the VP16-induced complex. Consistent with incorporation of the variously truncated HCF proteins in the VP16-induced complexes, the mobility of the complexes during electrophoretic mobility retardation varies with the size of the protein.

The results of HCF-VP16 association and VP16-induced complex formation with the HCF truncations, together with the kelch repeat similarity of the VP16-interacting region, indicate that VP16 binding and stabilization of the VP16-induced complex are both accomplished by a β-propeller-like

structure at the amino terminus of HCF. We refer to this region of HCF as the HCF_{VIC} domain.

The tsBN67 HCF point mutation lies in $HCF_{KEL}3$ and disrupts the association of HCF with VP16. The HCF_{VIC} domain spans the missense mutation P134S that causes the tsBN67 temperature-sensitive cell cycle arrest phenotype. The single tsBN67 proline-to-serine substitution lies within the third HCF_{KEL} repeat and changes one of the four positions that are conserved in all six HCF_{KEL} repeats (Fig. 2). We have previously shown that VP16 fails to activate transcription in tsBN67 cells at the nonpermissive temperature and that extracts from such cells fail to promote VP16-induced complex formation. In those studies, however, we could not distinguish between indirect effects on VP16 function due to arrest of tsBN67 cells at a phase of the cell cycle in which VP16 functions are normally not active and a direct effect of the P134S tsBN67 mutation on VP16 function (12). To distinguish between these possibilities, we directly tested the effect of the tsBN67 mutation on VP16-induced complex formation.

We compared the ability of the wild-type and P134S tsBN67 HCF_{VIC} domain synthesized in vitro to promote VP16-induced complex formation as shown in Fig. 5A. By translating the proteins in vitro, we could monitor their synthesis and stability. Figure 5A shows a comparison of the mobility of the VP16-induced complex formed with endogenous human HCF (lane 3) and the "mini"-VP16-induced complex formed by wild-type HCF_{N380} (lane 5) in an electrophoretic mobility retardation assay. HCF_{N380} carrying the P134S tsBN67 mutation, however, failed to promote VP16-induced complex formation (compare lanes 5 and 6). Thus, the tsBN67 HCF mutation has a direct effect on VP16-induced complex formation.

To determine whether the defect in VP16-induced complex formation coincides with loss of the interaction between the P134S tsBN67 HCF_{VIC} domain and VP16, we performed a coimmunoprecipitation experiment, whose results are shown in Fig. 5B. In reciprocal experiments, epitope-tagged wild-type and P134S HCF_{N380} were immunoprecipitated in the presence of untagged VP16 (lanes 1 and 2) and epitope-tagged VP16 was immunoprecipitated in the presence of untagged wild-type and P134S HCF_{N380} (lanes 3 and 4). In both cases, the P134S HCF_{N380} protein (lanes 2 and 4) bound VP16 10- to 20-fold less effectively than did the wild-type HCF_{N380} protein (lanes 1 and 3). These results suggest that the HCF tsBN67 cell cycle arrest mutation disrupts activation of transcription by VP16 in vivo, by disrupting the ability of HCF to associate with VP16, thus preventing the formation of the VP16-induced complex.

The HCF_{VIC} domain is sufficient to support VP16 transcriptional activation in vivo. Unlike animal cells, the yeast *S. cerevisiae* lacks HCF activity (40). We used the absence of HCF (and Oct-1 and VP16) activity in *S. cerevisiae* to assay the molecular requirements for activation of transcription by the VP16-induced complex in vivo. Figure 6 shows the results of such an experiment. We constructed a *S. cerevisiae* strain carrying an integrated *HIS3* gene with multiple VP16-responsive HSV TAATGARAT elements and full-length VP16, Oct-1 POU domain, and HCF_{N380} expression vectors. This strain grows in the presence (+his) or absence (−his) of histidine (sector A). The yeast cells, however, fail to grow in the absence of histidine, if (i) the *HIS3* gene lacks VP16-responsive TAAT GARAT elements (sector B), (ii) the Oct-1 POU domain carries a single-amino-acid substitution that prevents association with VP16 (E22A [19, 26]) (sector C), (iii) VP16 lacks its transcriptional activation domain (sector D), or (iv) HCF_{N380} either is left out (sector E) or carries the P134S tsBN67 point mutation (sector F), respectively. These results show that the HCF_{VIC} and Oct-1 POU domains are sufficient to support

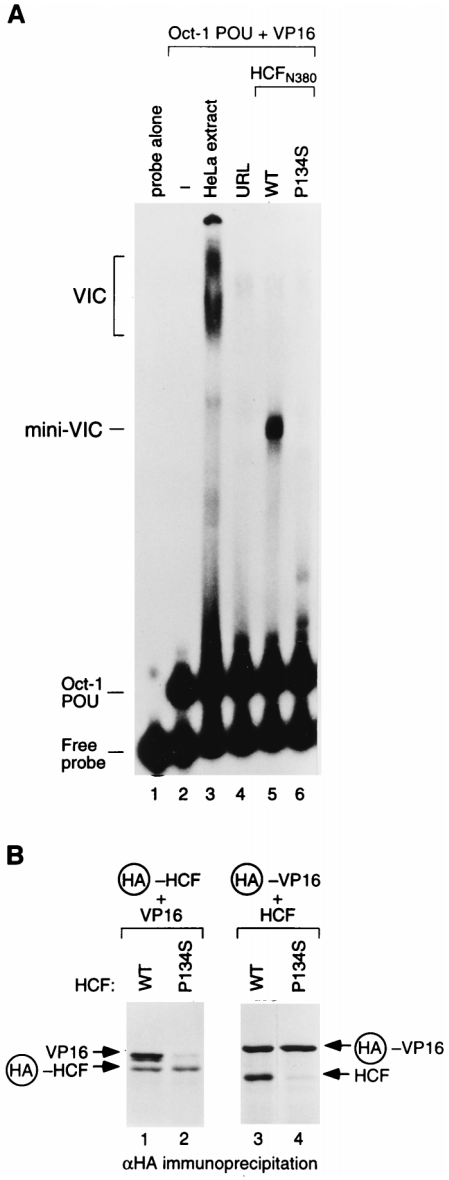

FIG. 5. The HCF tsBN67 point mutation disrupts stabilization of the VP16-induced complex and association with VP16. (A) HCF polypeptides were synthesized by translation in vitro and assayed for stabilization of the VP16-induced complex in an electrophoretic mobility retardation assay. Lane 1 contains probe alone, and lanes 2 to 6 contain probe with Oct-1 POU domain and GST-VP16 fusion protein: HeLa cell nuclear extract (lane 3), unprogrammed reticulocyte lysate (URL) (lane 4), and reticulocyte lysates programmed with templates for wild-type (WT; lane 5) or P134S tsBN67 (lane 6) human HCF_{N380}. The positions of the free probe, Oct-1 POU-domain complex, and VP16-induced complex containing native human HCF (VIC) or truncated HCF (mini-VIC) are indicated. (B) The P134S mutation disrupts the direct interaction between VP16 and HCF. Direct interaction between HCF_{N380} and VP16 was examined by coimmunoprecipitation assay as described in the legend to Fig. 3B. HA-tagged HCF_{N380} (WT) (lane 1) or HCF_{N380}P134S (lane 2) was mixed with untagged VP16ΔC, or, conversely, HA-tagged VP16ΔC was mixed with untagged HCF_{N380} (WT) (lane 3) or HCF_{N380}P134S (lane 4), and the mixtures were incubated prior to addition of the αHA antibody. Immune complexes were resolved on a 12% polyacrylamide gel and detected by fluorography.

VP16 transcriptional activation in vivo and that the interactions among members of the VP16-induced complex in *S. cerevisiae* are apparently specific, because individual point mutations in these two proteins that disrupt VP16-induced com-

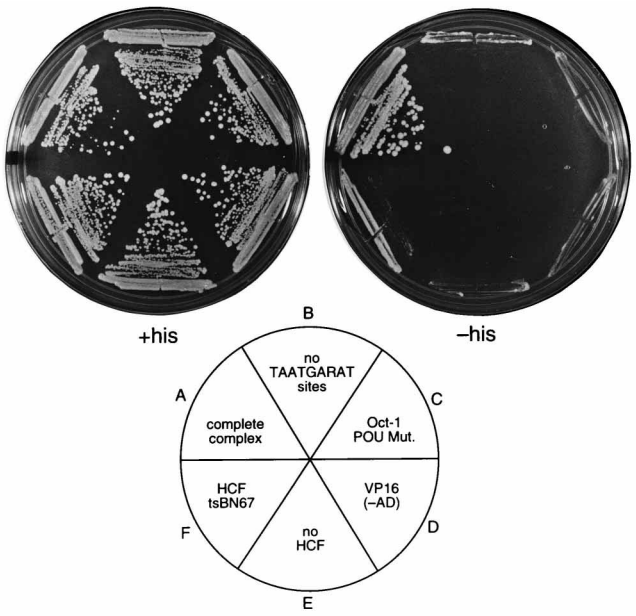

FIG. 6. The HCF_{VIC} domain is sufficient to promote VP16 activation of transcription in vivo. A yeast strain containing a *HIS3* reporter gene driven by six copies of an ($OCTA^+$)TAATGARAT element (A and C to F) or lacking the TAATGARAT element (B) was transformed with multiple yeast expression plasmids. Transformants were streaked on plates containing (+his) or lacking (−his) the amino acid histidine. The yeast cells were transformed with the following expression plasmids: segments A and B, HCF_{N380}, full-length VP16, and Oct-1 POU domain; segment C, HCF_{N380}, full-length VP16, and Oct-1 POU(E22A) domain; segment D, HCF_{N380}, VP16ΔC (lacking the carboxy-terminal transcriptional activation domain), and Oct-1 POU domain; segment E, full-length VP16 and Oct-1 POU domain; and segment F, HCF_{N380}P134S, full-length VP16, and Oct-1 POU domain.

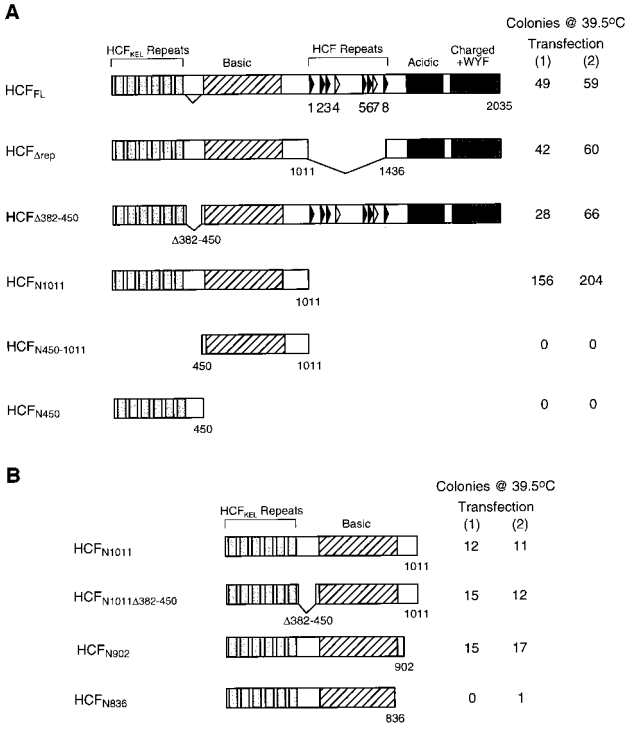

FIG. 7. Both the HCF_{VIC} domain and basic region are required to rescue the tsBN67 cell-proliferation defect. (A) Hamster tsBN67 cells were stably transfected with the pCGNHCF expression constructs indicated. Following transfection, the cells were incubated at 39.5°C with G418 for 2 weeks. The number of colonies scored in duplicate experiments is shown. (B) tsBN67 cells were transfected with the HCF expression constructs indicated and viable transformants at 39.5°C scored as in panel A. The results of duplicate experiments are shown.

plex formation in vitro also disrupt VP16 transcriptional activation in vivo.

The HCF_{VIC} domain is not sufficient to rescue the tsBN67 cell proliferation defect. The studies described above show that the amino-terminal HCF_{VIC} domain of HCF is sufficient to promote VP16-induced complex formation in vitro and transcriptional activation in vivo. In the experiment in Fig. 7, we determined the regions of HCF required to rescue the temperature-sensitive tsBN67 hamster cell defect. We transfected tsBN67 cells with a set of wild-type and truncated HCF expression vectors and assayed them for focus formation at 39.5°C, the nonpermissive temperature for tsBN67 cell proliferation. As described previously (12), full-length human HCF rescues the temperature-sensitive defect (Fig. 7A). Deletion of the HCF repeats ($HCF_{\Delta rep}$) does not disrupt the rescue of tsBN67 cells. This result shows that wild-type HCF need not be processed to complement the tsBN67 cell-proliferation defect. Furthermore, $HCF_{\Delta 382–450}$, in which amino-terminal and carboxy-terminal HCF fragment association is disrupted (41), complements the tsBN67 defect (Fig. 7A). Thus, amino-terminal and carboxy-terminal HCF-fragment association is not necessary to rescue the tsBN67 cell proliferation defect.

The amino-terminal half of HCF (HCF_{N1011}) also complements the tsBN67 cell proliferation defect, but when this region is divided in two, as in HCF_{N450} and $HCF_{N450–1011}$, neither fragment of HCF complements the tsBN67 cell defect (Fig. 7A). Thus, although the HCF_{VIC} domain can support VP16-induced complex formation and transcription, it is not sufficient to promote cell proliferation in tsBN67 cells; apparently, other amino-terminal HCF sequences are required. The deletion analysis shown in Fig. 7B suggests that the basic region of HCF acts cooperatively with the HCF_{VIC} domain to overcome the tsBN67 defect: neither deletion of the sequences between the two domains ($HCF_{N1011\Delta 382–450}$) nor deletion of sequences carboxy-terminal of the basic region (HCF_{N902}) affects tsBN67 cell complementation of the tsBN67 cell proliferation defect, but deletion of sequences extending into the basic region (HCF_{N836}) does disrupt complementation of the tsBN67-cell defect (Fig. 7B). Thus, the basic region of HCF provides an additional function that is required to overcome the tsBN67 cell proliferation defect but is not essential for VP16-induced complex formation. These results indicate that multiple regions of HCF are involved in promoting cell cycle progression, only one of which is targeted by VP16.

DISCUSSION

HCF, a cellular cofactor during HSV infection, is a structurally complex protein of more than 2,000 amino acids. We have identified the region of HCF responsible for stabilizing the HSV VP16-induced complex. This HCF_{VIC} domain is a relatively small region (361 amino acids) located at the amino terminus of the protein. Identification of this minimal domain indicates that despite its large size and complexity, only a small portion of HCF is intimately involved in stabilizing the VP16-induced complex. Mapping of the HCF_{VIC} domain to a small region of HCF suggests that assembly of the VP16-induced complex, a large multiprotein-DNA complex, results from the contributions of relatively small subdomains of the individual cellular components: Oct-1 provides the 160-amino-acid DNA-

binding POU domain (15, 30), and HCF provides the 361-amino-acid HCF_{VIC} domain (this study). These minimal domains of Oct-1 and HCF can support transcriptional activation by VP16 in vivo (Fig. 6); thus, the function, if any, of the other regions of Oct-1 and HCF in the regulation of HSV immediate-early gene transcription remains to be elucidated.

Specific proteolytic processing at the centrally located HCF repeats results in amino- and carboxy-terminal HCF fragments which remain associated with one another. Antibodies directed against the carboxy-terminal region of HCF disrupt VP16-induced complex formation (39), suggesting that the carboxy terminus of HCF is incorporated into the native complex. Although HCF processing and coassociation are conserved in mammals (9, 12), we show here that association of the HCF_{VIC} domain with the carboxy terminus of HCF is not required to stabilize the VP16-induced complex. Therefore, if other regions of HCF, including the carboxy terminus, play a role in stabilization of the VP16-induced complex, their role(s) is likely to be more subtle than that of the minimal HCF_{VIC} domain identified here.

The HCF_{VIC} domain is likely to form a six-bladed β-propeller. The amino acid sequence of the HCF_{VIC} domain contains six copies of a repeat motif related to repeats found in other proteins, including the *Drosophila* egg chamber protein Kelch (45), and these repeats are likely to form a β-propeller structure (3). A β-propeller can contain four to eight circularly arranged β-sheets, forming β-propellers with four to eight blades (13, 23, 34, 43). Each of the six HCF_{KEL} repeats is predicted to form a β-sheet, thus forming a six-bladed β-propeller structure. The proposed β-propeller structure coincides precisely with the HCF_{VIC} domain (Fig. 4), suggesting that the integrity of this structure is required for HCF to bind VP16 and stabilize the VP16-induced complex. Consistent with this conclusion, individual triple-alanine-substitution mutations of the conserved FGG sequence in repeats $HCF_{KEL}1$ and $HCF_{KEL}3$ and the corresponding WSG sequence in the $HCF_{KEL}6$ repeat disrupt VP16-induced complex assembly (10). As indicated in Fig. 2, these residues are predicted to lie at the end of the second β-strand and are expected to play a critical role in maintenance of the β-propeller fold.

The β-propeller structure is a common structural motif shared by many proteins with different functions and little sequence similarity. The crystal structures of a number of disparate enzymes including influenza virus neuraminidase, a six-bladed β-propeller (34), and fungal galactose oxidase, a seven-bladed β-propeller (13), have been solved. In these enzymes, the active site is composed of loops between β-strands arranged on one surface of the propeller. Thus, the β-sheets that form the propeller blades generate an apparent scaffold upon which structural and functional specificity is built.

Perhaps the β-propeller structure most relevant to the HCF_{VIC} domain and its interaction with VP16 is that of the β subunit of the heterotrimeric G proteins (22, 28, 36). Heterotrimeric G proteins are the regulatory target of seven-helix transmembrane receptors (6). They are composed of three molecules: a G_α subunit and a stable heterodimer of G_β and G_γ subunits. The G_β subunit contains a seven-bladed β-propeller that binds to the G_α subunit, thus coordinating protein complex assembly (22, 36).

It is not known how HCF associates with VP16 and stimulates VP16-induced complex formation. One hypothesis is that HCF binds to and stabilizes a conformation of VP16 that can associate more effectively with Oct-1 and TAATGARAT regulatory sites (17). The structure of the heterotrimeric G-protein complex provides evidence for such conformation-specific interactions with a β-propeller structure because only one of multiple known G_α subunit conformations —the GDP-bound form — binds to the G_β β-propeller structure (22, 36). Thus, in the same way that the G_β subunit associates with a specific conformation of the G_α subunit, the HCF_{VIC} domain may associate with and then stabilize a specific conformation of VP16.

Stabilization of such a specific conformation of VP16 by HCF may involve more than simply binding of HCF to VP16. Simmen et al. (27) have performed a mutational analysis of the HCF_{VIC} domain described here. Substitution of HCF residues E102 and K105 affected VP16-induced complex assembly. These residues lie within the $HCF_{KEL}2$ repeat, near the tsBN67 P134S mutation in the $HCF_{KEL}3$ repeat (Fig. 2). However, in contrast to the tsBN67 mutation which disrupts HCF binding to VP16, the two $HCF_{KEL}2$ repeat mutations have no evident effect on HCF binding to VP16. Together, these results suggest that P134 lies at or near a critical contact surface between HCF and VP16, whereas the nearby residues E102 and K105 affect a separate function of HCF involved in promoting the formation of the VP16-induced complex, perhaps through stabilization of a specific conformation of VP16 (27).

VP16 targets a region of HCF involved in cell cycle progression. The tsBN67 mutation in HCF causes a temperature-sensitive G_0/G_1 cell cycle arrest (12). We have shown here that this single point mutation is located in the HCF_{VIC} domain and disrupts the ability of HCF to bind VP16, stabilize the VP16-induced complex, and activate transcription in vivo. Thus, VP16 apparently targets a surface of HCF used to promote cell proliferation. We believe that, to interact with HCF, VP16 mimics a cellular protein whose natural function involves association with HCF to promote cell cycle progression. If this is true, the interaction between VP16 and HCF would serve as an excellent sensor of the cell cycle status of the infected cell, allowing VP16 to coordinate initiation of the lytic phase of the virus life cycle with the cell cycle status of the infected cell.

Efficient rescue of the tsBN67 phenotype requires more than the HCF_{VIC} domain: the adjoining basic region is also required. Thus, both Oct-1 and HCF display different requirements for their HSV-associated and cellular functions. The Oct-1 POU domain and HCF_{VIC} domain are sufficient to promote the activation of transcription by VP16 (7) (see above), but additional domains, transcriptional activation domains in Oct-1 (31) and the basic region in HCF (this study), are involved in the cellular functions of Oct-1 and HCF, respectively. The identification of cellular effector molecules responsible for the functions of HCF will be important for illuminating how HCF promotes cell cycle progression.

ACKNOWLEDGMENTS

We thank D. Aufiero for technical assistance and DNA sequencing; C. Alexandre and M. Gilman for *S. cerevisiae* expression vectors; W. Tansey for pNCITE; J. Chong and G. Mandel for the *S. cerevisiae* integration vector pTH1; J. Duffy, M. Ockler, and P. Renna for artwork; and W. Tansey for critical comments on the manuscript.

A.C.W. was supported in part by a Damon Runyon-Walter Winchell Cancer Research Fund Fellowship (DRG-1073). These studies were supported by U.S. Public Health Service grants CA-13106 and GM54598.

REFERENCES

1. **Alexandre, C., D. A. Grueneberg, and M. Z. Gilman.** 1993. Studying heterologous transcription factors in yeast. Methods **5:**147–155.
2. **Boeke, J. D., J. Trueheart, G. Natsoulis, and G. R. Fink.** 1987. 5-Fluoroorotic acid as a selective agent in yeast molecular genetics. Methods Enzymol. **154:**164–175.
3. **Bork, P., and R. F. Doolittle.** 1994. Drosophila kelch motif is derived from a common enzyme fold. J. Mol. Biol. **236:**1277–1282.
4. **Branden, C., and J. Tooze.** 1991. Introduction to protein structure. Garland Inc., New York, N.Y.

5. **Chong, J. A., J. Tapia-Ramirez, S. Kim, J. J. Toledo-Aral, Y. Zheng, M. C. Boutros, Y. M. Altshuller, M. A. Frohman, S. D. Kraner, and G. Mandel.** 1995. REST: a mammalian silencer protein that restricts sodium channel gene expression to neurons. Cell **80:**949–957.
6. **Clapham, D. E.** 1996. The G-protein nanomachine. Nature **379:**297–299.
7. **Cleary, M. A., S. Stern, M. Tanaka, and W. Herr.** 1993. Differential positive control by Oct-1 and Oct-2: activation of a transcriptionally silent motif through Oct-1 and VP16 corecruitment. Genes Dev. **7:**72–83.
8. **Eichinger, L., L. Bomblies, J. Vandekerckhove, M. Schleicher, and J. Gettemans.** 1996. A novel type of protein kinase phosphorylates actin in the actin-fragmin complex. EMBO J. **15:**5547–5556.
9. **Frattini, A., A. Chatterjee, S. Faranda, M. G. Sacco, A. Villa, G. E. Herman, and P. Vezzoni.** 1996. The chromosome localization and the HCF repeats of the human host cell factor gene (HCFC1) are conserved in the mouse homologue. Genomics **32:**277–280.
10. **Freiman, R. N., A. C. Wilson, and W. Herr.** Unpublished results.
11. **Gerster, T., and R. G. Roeder.** 1988. A herpesvirus transactivator protein interacts with transcription factor OTF-1 and other cellular proteins. Proc. Natl. Acad. Sci. USA **85:**6347–6351.
12. **Goto, H., S. Motomura, A. C. Wilson, R. N. Freiman, Y. Nakabeppu, K. Fukushima, M. Fujishima, W. Herr, and T. Nishimoto.** 1997. A single-point mutation in HCF causes temperature-sensitive cell-cycle arrest and disrupts VP16 function. Genes Dev. **11:**726–737.
13. **Ito, N., S. E. V. Phillips, K. D. S. Yadav, and P. F. Knowles.** 1994. Crystal structure of a free radical enzyme, galactose oxidase. J. Mol. Biol. **238:**794–814.
14. **Katan, M., A. Haigh, C. P. Verrijzer, P. C. Van der Vliet, and P. O'Hare.** 1990. Characterization of a cellular factor which interacts functionally with Oct-1 in the assembly of a multicomponent transcription complex. Nucleic Acids Res. **18:**6871–6880.
15. **Kristie, T. M., J. H. LeBowitz, and P. A. Sharp.** 1989. The octamer-binding proteins form multi-protein-DNA complexes with the HSV αTIF regulatory protein. EMBO J. **8:**4229–4238.
16. **Kristie, T. M., J. L. Pomerantz, T. C. Twomwey, S. A. Parent, and P. A. Sharp.** 1995. The cellular C1 factor of the herpes simplex virus enhancer complex is a family of polypeptides. J. Biol. Chem. **270:**4387–4394.
17. **Kristie, T. M., and P. A. Sharp.** 1990. Interactions of the Oct-1 POU subdomains with specific DNA sequences and with the HSV α-*trans*-activator protein. Genes Dev. **4:**2383–2396.
18. **Kristie, T. M., and P. A. Sharp.** 1993. Purification of the cellular C1 factor required for the stable recognition of the Oct-1 homeodomain by the herpes simplex virus α-trans-induction factor (VP16). J. Biol. Chem. **268:**6525–6534.
19. **Lai, J.-S., M. A. Cleary, and W. Herr.** 1992. A single amino acid exchange transfers VP16-induced positive control from Oct-1 to the Oct-2 homeo domain. Genes Dev. **6:**2058–2065.
20. **Lai, J.-S., and W. Herr.** 1992. Ethidium bromide provides a simple tool for identifying genuine DNA-independent protein associations. Proc. Natl. Acad. Sci. USA **89:**6958–6962.
21. **Lai, J.-S., and W. Herr.** 1997. Interdigitated residues within a small region of VP16 interact with Oct-1, host cell factor, and DNA. Mol. Cell. Biol. **17:** 3937–3946.
22. **Lambright, D. G., J. Sondek, A. Bohm, N. P. Skiba, H. E. Hamm, and P. B. Sigler.** 1996. The 2.0 Å crystal structure of a heterotrimeric G protein. Nature **379:**311–319.
23. **Murzin, A. G., A. M. Lesk, and C. Chothia.** 1994. Principles determining the structure of beta-sheet barrels in proteins. II. The observed structures. J. Mol. Biol. **236:**1382–1400.
24. **Nishimoto, T., and C. Basilico.** 1978. Analysis of a method for selecting temperature sensitive mutants of BHK cells. Somatic Cell Genet. **4:**323–340.
25. **O'Hare, P.** 1993. The virion transactivator of herpes simplex virus. Semin. Virol. **4:**145–155.
26. **Pomerantz, J. L., T. M. Kristie, and P. A. Sharp.** 1992. Recognition of the surface of a homeo domain protein. Genes Dev. **6:**2047–2057.
27. **Simmen, K. A., A. Newell, M. Robinson, J. S. Mills, G. Canning, R. Handa, K. Parkes, N. Borkakoti, and R. Jupp.** 1997. Protein interactions in the herpes simplex virus type 1 VP16-induced complex: VP16 peptide inhibition and mutational analysis of host cell factor requirements. J. Virol. **71:**3886–3894.
28. **Sondek, J., A. Bohm, D. G. Lambright, H. E. Hamm, and P. B. Sigler.** 1996. Crystal structure of a G_A protein βγ dimer at 2.1 Å resolution. Nature **379:**369–374.
29. **Springer, T. A.** 1997. Folding of the N-terminal, ligand-binding region of integrin α-subunits into a β-propeller domain. Proc. Natl. Acad. Sci. USA **94:**65–72.
30. **Stern, S., M. Tanaka, and W. Herr.** 1989. The Oct-1 homeodomain directs formation of a multiprotein-DNA complex with the HSV transactivator VP16. Nature **341:**624–630.
31. **Tanaka, M., J.-S. Lai, and W. Herr.** 1992. Promoter-selective activation domains in Oct-1 and Oct-2 direct differential activation of an snRNA and mRNA promoter. Cell **68:**755–767.
32. **Thomas, B. J., and R. Rothstein.** 1989. Elevated recombination rates in transcriptionally active DNA. Cell **56:**619–630.
33. **Thompson, C. C., and S. L. McKnight.** 1992. Anatomy of an enhancer. Trends Genet. **8:**232–236.
34. **Varghese, J. N., W. G. Laver, and P. M. Colman.** 1983. Structure of the influenza virus glycoprotein antigen neuraminidase at 2.9 Å resolution. Nature **303:**35–40.
35. **Varkey, J. P., P. J. Muhlrad, A. N. Minniti, B. Do, and S. Ward.** 1995. The Caenorhabditis elegans spe-26 gene is necessary to form spermatids and encodes a protein similar to the actin-associated proteins kelch and scruin. Genes Dev. **9:**1074–1086.
36. **Wall, M. A., D. E. Coleman, E. Lee, J. A. Iniguez-Lluhi, B. A. Posner, A. G. Gilman, and S. R. Sprang.** 1995. The structure of the G protein heterotrimer $G_{ia1}\beta_1\gamma_2$. Cell **83:**1047–1058.
37. **Watanabe, M., N. Furuno, M. Goebl, M. Go, K. Miyauchi, T. Sekiguchi, C. Basilico, and T. Nishimoto.** 1991. Molecular cloning of the human gene, CCG2, that complements the BHK-derived thermosensitive cell cycle mutant tsBN63: identity of CCG2 with the human X chromosomal SCAR/RPS4X gene. J. Cell Sci. **100:**35–43.
38. **Way, M., M. Sanders, C. Garcia, J. Sakai, and P. Matsudaira.** 1995. Sequence and domain organization of scruin, and actin-crosslinking protein in the acrosomal process of Limulus sperm. J. Cell Biol. **128:**51–60.
39. **Wilson, A. C., K. LaMarco, M. G. Peterson, and W. Herr.** 1993. The VP16-accessory protein HCF is a family of polypeptides processed from a large precursor protein. Cell **74:**115–125.
40. **Wilson, A. C., M. A. Cleary, J.-S. Lai, K. LaMarco, M. G. Peterson, and W. Herr.** 1993. Combinatorial control of transcription: the herpes simplex virus VP16-induced complex. Cold Spring Harbor Symp. Quant. Biol. **58:**167–178.
41. **Wilson, A. C., M. G. Peterson, and W. Herr.** 1995. The HCF repeat is an unusual proteolytic cleavage signal. Genes Dev. **9:**2445–2458.
42. **Wilson, A. C., and W. Herr.** Unpublished results.
43. **Xia, Z.-X., W.-W. Dai, J.-P. Xiong, Z.-P. Hao, V. L. Davidson, S. White, and S. F. Mathews.** 1992. The three-dimensional structure of methanol dehydrogenase from two methylotrophic bacteria at 2.6-Å resolution. J. Biol. Chem. **267:**22289–22297.
44. **Xiao, P., and J. P. Capone.** 1990. A cellular factor binds to the herpes simplex virus type 1 transactivator Vmw65 and is required for Vmw65-dependent protein-DNA complex assembly with Oct-1. Mol. Cell Biol. **10:**4974–4977.
45. **Xue, F., and L. Cooley.** 1993. Kelch encodes a component of intercellular bridges in Drosophila egg chambers. Cell **72:**681–693.